MORPHOLOGICAL AND CHEMICAL FEATURES OF BIOWEATHERED GRANITIC BIOTITE INDUCED BY LICHEN ACTIVITY

Jacek Wierzchos† and Carmen Ascaso

Centro de Ciencias Medioambientales, CSIC, Serrano 115 dpdo., 28006 Madrid, Spain

† Servicio de Microscópia Electrónica, Universitat de Lleida, Rovira Roure 44, 25196 Lleida, Spain

Abstract—to study the physico-chemical activity of lichens on micaceous components of granitic rocks, samples covered by thalli of *Parmelia conspersa* (Ehrht) Ach. and *Aspicilia intermutans* (Nyl.) Arn. were collected and examined with Scanning Electron Microscopy (SEM) equipped with a Back Scattered Electron (BSE) detector and an Energy Dispersive Spectroscopy (EDS) microanalytical system. The biophysical activity of both lichen species leads to a deep alteration of biotite, which results in detachment, separation and exfoliation of biotite plates. Chemically, the bioweathering process of biotite in the lichen-mineral contact zone involves considerable depletion of potassium (K) from interlayer positions in biotite and removal of several elements, corresponding to a 9.7% loss in matter. The sequence of the loss of elements is: $K^+ \gg Fe^{tot} > Ti^{4+} \cong Mg^{2+}$. There are also some gains in the order: $Ca^{2+} > Na^+ \gg Al^{3+} > Si^{4+}$ attributed to dissolution of co-existing Ca and Na rich minerals. Geochemical mass balance results suggest the transformation of K-rich biotite to scarcely altered biotite interstratified with a biotite-vermiculite intermediate phase in the lichen bioweathered contact zones.

Key Words—*Aspicilia intermutans,* Biotite, Bioweathering, Granite, Lichens, *Parmelia conspersa.*

INTRODUCTION

The role of physical and chemical factors in the weathering of micaceous minerals has been adequately documented. A common biotite weathering route is the suppression of K release due to oxidation during synthetic degradation processes (Barshad and Kishk 1968; Rich 1972; Gilkes 1973; Gilkes et al. 1973; Ross and Rich 1974; Goulding 1983; Scott and Amonette 1988; Dreher and Niederbudde 1994). In those laboratory experiments biotite altered to vermiculite and/or mixed-layer clay minerals. Natural weathering of biotite may also produce kaolinite, halloysite, illite, smectite, chlorite and sesquioxides (Stoch and Sikora 1976; Gilkes and Suddhiprakarn 1979; Craw et al. 1982; White et al. 1985; AlDahan and Morad 1986; Morad 1990; Robertson and Eggleton 1991). In contrast to the abundant data on synthetic and natural physico-chemical weathering of micaceous minerals, the involvement of biological alteration processes is not as well understood. Lichens commonly occur on rocks, both in their natural state and also when used as monumental and building stones. Thus, lichen-encrusted rocks provide an ideal environment for studying biological aspects of mineral weathering. The first studies of lichen weathering of rocks led to the conclusion that the effect might almost be entirely ascribed to physical causes. It is known today that the lichen-rock interface is a place of considerable chemical activity, due to extracellular excretion of organic acids and organic compounds with chelating capacity (Jones and Wilson 1985). Biotite bioweathering is of great importance to the study of pedogenetic processes. Biotite bioweathering is important, both for under-standing pedogenetic processes and biodeterioration of granitic monumental and building stones. Few works have investigated the morphological and chemical features affecting biotite during biochemical weathering induced by lichens. Iskandar and Syers (1972), in laboratory experiments studying metal-complex formation by lichen acids with aqueous suspensions of biotite, granite and basalt observed release of Fe, Al, Ca and Mg from silicates. Chelating properties of lichen acids were investigated later by Ascaso et al. (1976) and Ascaso and Galvan (1976) who reacted mica and other minerals with suspended lichens. Those laboratory works demonstrated that lichens could alter their mineral substrates and provided strong circumstantial evidence that this alteration was mediated by the activity of specific lichens. It was concluded that lichens that produce lichen acids could be significant weathering agents in nature. Depletion of Mg, Fe, K and Al on the mica surface was reported only one time by Wilson and Jones (1983) for naturally lichenized granite.

Given that activities of at least some lichens could lead to deterioration of their immediate micaceous substrates, the question is raised as to the exact nature of the processes involved and to the tendency of mineral transformation in natural conditions.

The aim of this work was to: 1) improve the knowledge of natural biological weathering processes of the micaceous component of granitic rocks; and 2) identify pathways for the morphological and chemical changes of biodegraded granitic biotite.

MATERIALS AND METHODS

Pieces of granitic rock covered by the foliose thallus of *Parmelia conspersa* (Ehrht) Ach. and crustose *As-*

picilia intermutans (Nyl.) Arn. and coexisting pieces without lichen cover were collected at Bustarviejo de la Sierra, near Madrid. Previous petrographic and X-ray diffraction (XRD) studies of this material showed the presence of quartz, orthoclase and plagioclase in the granitic rock as major rock-forming minerals, and biotite, zircon and apatite as accessory minerals (Ascaso 1985). Part of lichen-colonized rocks was processed according to conventional transmission electron microscopy (TEM) procedures for the preparation of lichen material (Ascaso et al. 1986) applying LR White resin as the impregnate medium. Afterward, the blocks were cut and fine polished. Wierzchos and Ascaso (1994) give detailed information concerning this preparation technique. Those samples were then examined with SEM in backscattered electron (BSE) emission mode using a DSM 960 Zeiss apparatus. The subsequent microprobe analysis as points analysis, spatial element distribution and microprobe profile with Energy Dispersive Spectrometry (EDS) Link ISIS microanalytical system were made on the SEM-BSE samples simultaneously during SEM observation operating at a 35° take-off angle, an accelerating voltage of 15 kV, a working distance of 25 mm and a specimen current of 1–5 nA. Quantitative mineral analyses were obtained using standard ZAF correction procedures. Muscovite was used as a reference to standardize the analysis condition.

Taking into account multipoint EDS analyses performed on SEM-BSE samples, the geochemical mass balance of the major elements was calculated by the Barth method (1948). The number of ions contained within a single unit cell network based on 22 O atoms has also been transformed into the weights of the corresponding elements and the loss, or gain, of each element, and the total loss of matter has thus been obtained (Lineares et al. 1987; Pozzuoli et al. 1994).

RESULTS

Scanning Electron Microscopy Observations

The SEM-BSE micrographs of lichen-micaceous material obtained from transverse sections across the lichen-mineral interface (Figure 1) show various aspects of biophysico-chemical weathering of granitic biotite. Figure 1a (general view) and Figure 1b (detail view) and Figure 1c demonstrate the *P. conspersa* biotite interface. Successive detachment and separation of biotite was observed in lichen-micaceous mineral contact zones. An abundance of hyphae masses between biotite sheets were apparent. As the BSE signal is strongly dependent upon mean atomic number of the target (Joy 1991) it was possible to observe different levels of grey in the bioweathered biotite sheets (Figure 1b). Particularly the exfoliated sheets demonstrate a deeper shade of grey, indicating the mean

atomic number in this zone was less than in the coexisting unaffected one.

Similar exfoliation of biotite was also observed for the case of granitic mica covered by crustose *A. intermutans* (Figures 1d and 1e). Some biotite particles were curved (Figure 1d; lower left part) and others were detached and surrounded by fungal hyphae (Figure 1e). Figure 1f demonstrates the physical action of *A. intermutans* hyphae packed into a deep fissure (3 mm below surface) between biotite sheets. Detachment of biotite plates from fissure walls was observed.

Microprobe Examinations

In Figure 2, EDS X-ray images demonstrate the spatial distribution of Fe and K on bioweathered biotite. The Fe spatial distribution maps exactly record the forms and shapes of micaceous material shown on the BSE images (Figures 1b, 1d, 1e, 1f). However, an evident lack of K in the biotite sheets attached to the hyphae cells was observed. Figure 2a shows a large, approximately 350 μm, K-depletion zone in the central part of the exfoliated granitic biotite. The K-depletion effect observed in Figures 2b and 2c occurred more intensively in the approximate area of cracks and narrow fissures between separated biotite layers. The next Fe and K distribution maps (Figure 2d) were taken in the fissure filled with hyphae, which occur at 3 mm distance from the granitic rock surface. Loss of K was observed in detached packets of biotite layers and also in the fissure walls zones. In the case of finely exfoliated biotite layers as shown in the BSE image (Figure 1c), K-depletion can be easily demonstrated by the EDS microprobe line profile (Figure 3). The relative concentration of Al was more or less constant (Figure 1c line), and a slight decrease of Fe was observed in separated biotite layers. However, the relative concentration of K was distinctly smaller for exfoliated biotite sheets. The substraction of microprobe line profile for Fe and for K shown in the bottom of Figure 3, indicates sites of K release occurring in separated biotite plates.

EDS microanalysis also permits determination of chemical and mineralogical features within bioweathered biotite. Multipoint EDS analyses from the unaffected K-rich zone (white shade) and from the coexisting, K-depleted (grey shade on the BSE image—Figure 1b) area were performed. Results of quantitative analyses as wt% of oxides and calculation of structural formulae on the basis of 22 oxygens per unit cell are displayed in Table 1. Moreover, results of the geochemical mass balance, based upon EDS data for major elements for both examined zones are set out in Table 2. Quantitatively, the percentage of element losses during bioweathering ($1 \rightarrow 2$) was $K^+ \gg Fe^{tot} > Ti^{4+} \cong Mg^{2+}$ with total losses of mass on bioweathered biotite 47.7 g/22 O. The gain sequence was $Ca^{2+} > Na^+ \gg Al^{3+} > Si^{4+}$. Nevertheless, changes in mass
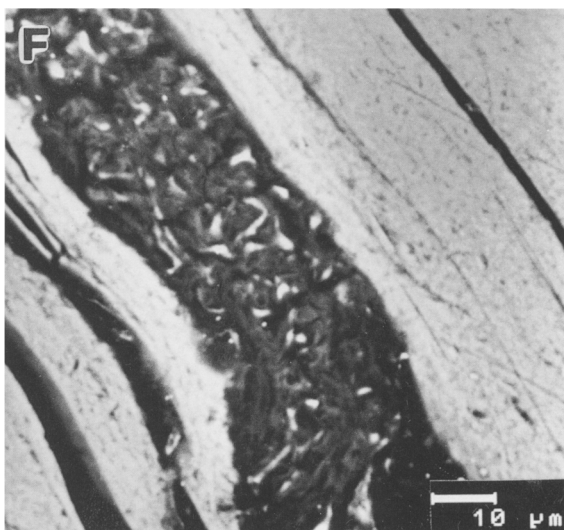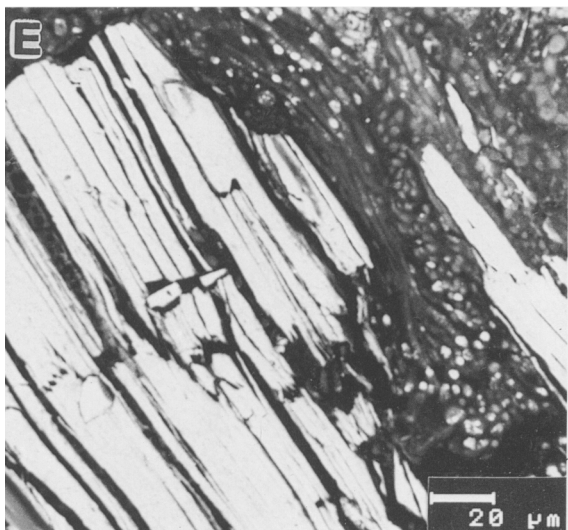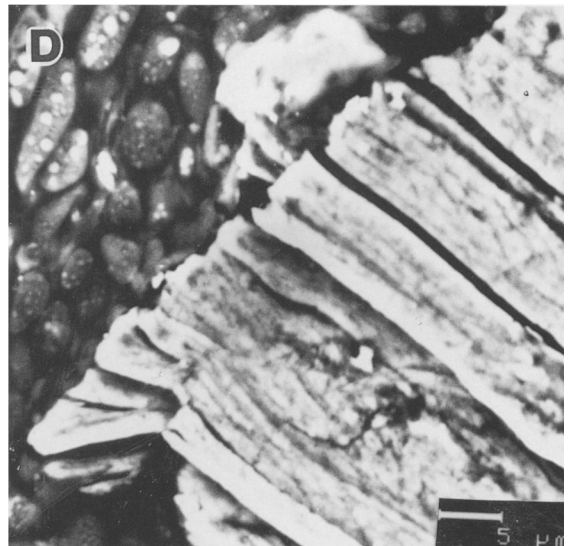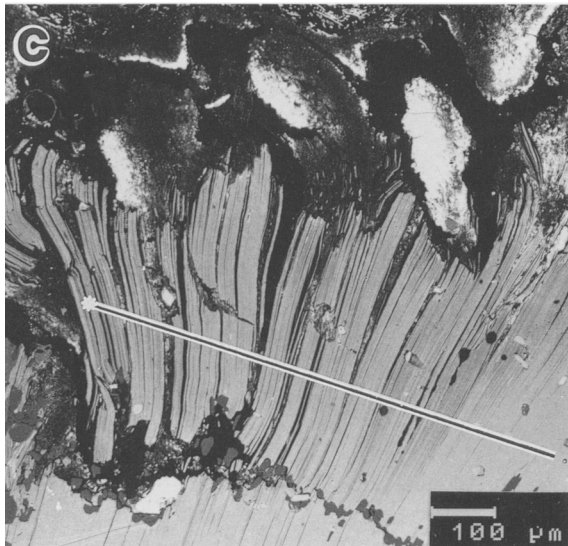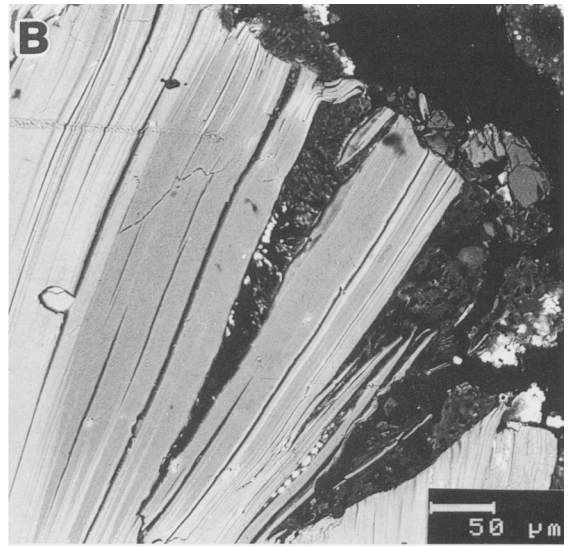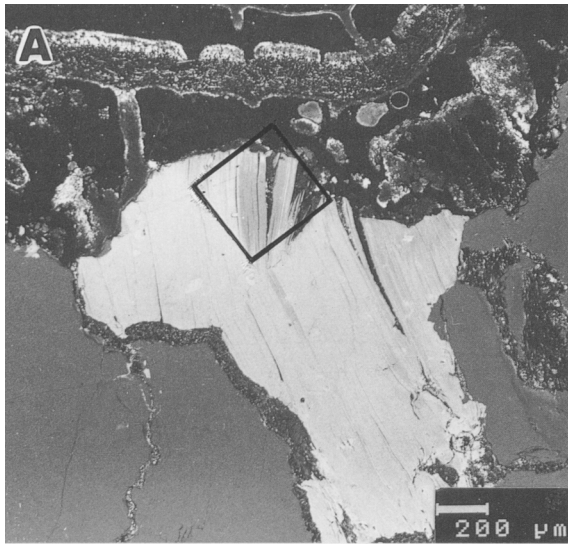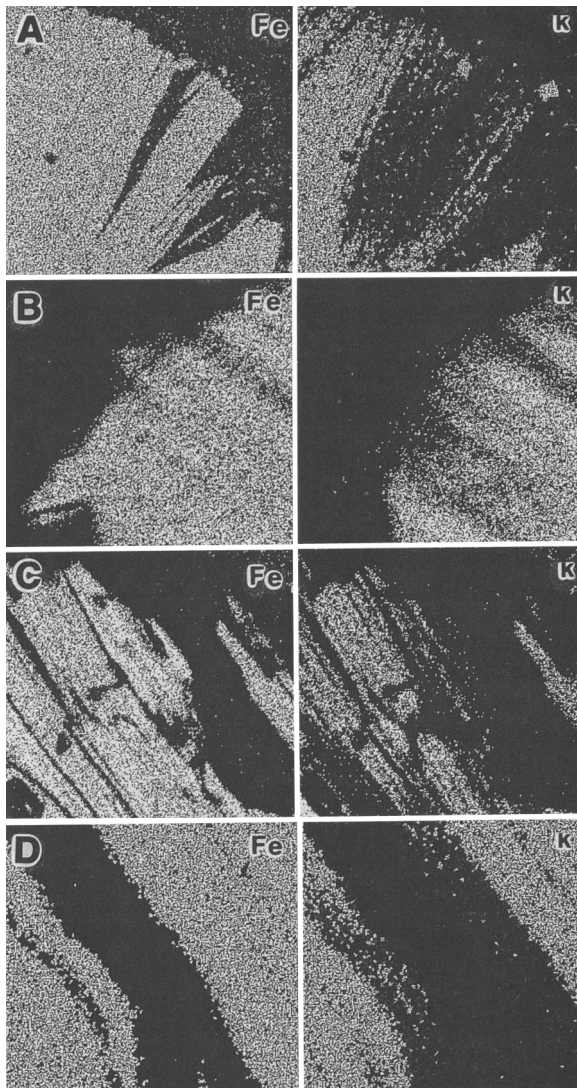
Figure 2.   Elemental spatial distribution of Fe and K. 2a, 2b, 2c and 2d correspond to Figures 1b, 1d, 1e and 1f respectively. EDS measurements.

Figure 3.   Microprobe line profile across line drawn in Figure 1c. EDS measurement.

DISCUSSION AND CONCLUSIONS

Detachment, separation and exfoliation of granitic biotite plates in adhesion zones of epilithic foliose and crustose lichen thalli confirm the strong physical action of lichens. Similar biophysical effects of the endolithic *Lecidea auriculata* thallus were also observed by Ascaso and Wierzchos (1994). Hyphae penetration and expansion and contraction processes generated by alternate wetting and drying cycles led to biophysical weathering of biotite. Chemical changes demonstrated by microprobe analyses also suggest biochemical weathering of biotite. Lichen thalli can form characteristic chemical microenvironment and specific weathering conditions (microclimate) affecting the immediate substratum surface. Syers and Iskandar (1973) suggested 3 possible processes for such bioweathering effects involving carbonic acids, lichen acids and oxalic acids. The possible mechanisms and results of chemical action of these lichenic substances as acid attack and/or chelating effects have been discussed in detail by Jones and Wilson (1985) and Wilson (1995). However, those authors concluded that these processes had not been conclusively demonstrated in natural samples. In this work, distinct depletion of interlami-

of Ti^{4+}, Mg^{2+} and Si^{4+} contents were insignificant, indicating that these elements were conserved during bioalteration. We also examined biotite grains with no lichen cover on the surface or fissures with SEM-BSE and EDS. These zones lacked characteristic bioalteration features.
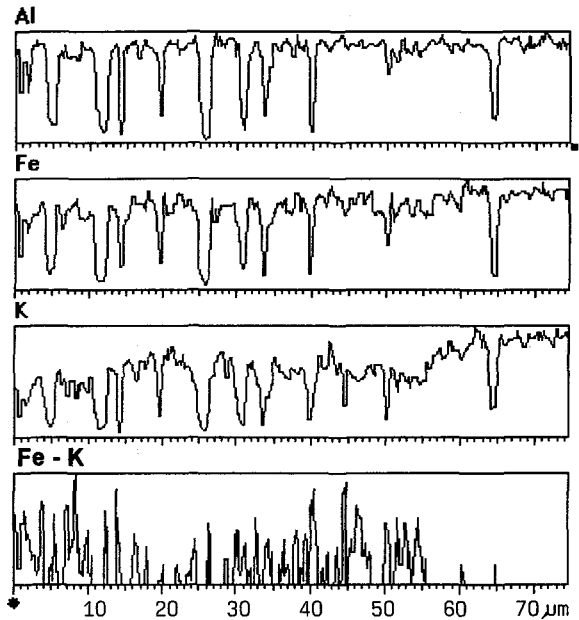
←

Figure 1.   SEM-BSE images of the lichen-granitic biotite contact zone. Figures 1a and 1c: general view of the *Parmelia conspersa*-biotite interface. Key: T = thallus; A = algal layer; m = medulla. Arrows indicates rhizine in longitudinal section (R) and fragments of rhizine (r) attached to biotite (B). Figure 1b: detail of Figure 1a. Figures 1d and 1e: interface zone between the *Aspicilia intermutans* thallus and biotite sheets. Key: H = hyphae. Figure 1f: fissure in the biotite grain filled by hyphae (H).

Table 1. Comparison of elemental composition between co-existing K-rich (white part) and K-poor (gray part) zones of the biotite shown in Figure 1b. (Oxide wt%; FeO[1] represents total Fe).

	K-rich (16 analyses)		K-poor (14 analyses)	
	Mean	Std. dev.	Mean	Std. dev.
SiO_2	38.17	0.57	40.56	0.31
TiO_2	2.34	0.23	2.32	0.07
Al_2O_3	16.57	0.18	22.54	0.23
FeO[1]	25.08	0.29	22.70	0.37
MnO	0.60	0.09	0.62	0.14
MgO	7.72	0.21	8.28	0.26
Na_2O	0.33	0.04	1.51	0.05
K_2O	8.12	0.40	1.11	0.10
CaO	0.07	0.01	0.37	0.04
Elem. ratios based on 22 O				
Tet. Si	5.36		5.38	
Al	2.64		2.62	
Oct. Al	0.10		0.90	
Fe[tot]	2.75		2.27	
Mg	1.67		1.64	
Mn	0.08		0.08	
Ti	0.25		0.24	
Large cations				
Ca	0.01		0.05	
Na	0.09		0.39	
K	1.46		0.19	

Table 2. Geochemical mass balance of the K-rich (1) and K-poor (2) biotite zones according to results shown in Table 1.

	Element (g)/22 O		Element loss (%)
	1	2	1 → 2
Si	150.6	151.2	0.4†
Al[tot]	74.0	95.0	28.3†
Fe[tot]	153.7	126.8	17.5
Mg	40.1	39.3	2.0
Mn	4.4	4.4	0
Ti	12.0	11.5	4.2
Ca	0.4	2.0	400.0†
Na	2.1	8.9	323.8†
K	56.9	7.4	86.9
Sum	494.2	446.5	
Total losses (%)			9.7

† Gain.

The geochemical mass balance data showed in Table 2 indicates that loss of Fe as total Fe was observed. The application of microprobe analysis does not permit determination of the valence of the Fe cations, but according to Pozzuoli et al. (1994) more intensive decreases in Fe^{2+} than gains in Fe^{3+} during the first stage of natural weathered biotite can be suspected. Moreover, an increase in Ca^{2+} and Na^+ in the interlaminar spacing was observed. This gain is probably due to the dissolution of fragments of coexisting Ca and Na rich (apatite and feldspars) minerals in the granitic rock and deposition of these cations in interlaminar spaces.

As has been shown by Mortland et al. (1956), biotite can alter to vermiculite if interlayer K is used as a nutritional source by plants. The transformation of mica into vermiculite has been observed in laboratory experiments by Weed et al. (1969) as a result of K exchange by cations present in nutrient solution, and soil fungi shifted the equilibrium in this reaction by absorption of K^+ cations. According to recent studies carried out by Pozzuoli et al. (1994), natural weathering of biotite to vermiculite occurred in a localized and heterogeneous way. These authors found out that even small samples are normally characterized by different spatial concentrations of biotite, vermiculite and an intermediate interstratified phase in dependency to the alteration grade. Our results for the geochemical mass balance (Table 2) as element losses or gains and total loss of mass of the bioweathered biotite zone were in good agreement with data obtained by Pozzuoli et al. (1994) and suggest the transformation biotite to scarcely altered biotite with a biotite-vermiculite intermediate interstratified phase. However, additional work remains to be done to confirm the occurrence of this mineralogical transformation of biotites in the lichen-mineral interface. Nevertheless, it is reasonable to conclude that the physico-chemical action of lichens can accelerate weathering rates of biotite.

nar K in adhesion zones of *P. conspersa* and *A. intermutans* thalli, on granitic biotite sheets was observed. Moreover, suppression of K release was also noted at the edge between biotite grain and hyphae cells in the deep fissure (Figures 1f; 2d). The formation of K-depleted biotite in natural and/or laboratory weathering is a well-known process (Rich 1972; Gilkes 1973; Goulding 1983; Dreher and Niederbudde 1994). Generally, these workers concluded that oxidation of Fe and subsequent reactions to maintain electro-neutrality produce biotites with K-release properties. According to Reichenbach and Rich (1969) initial exchange of K^+ may be affected more easily by a complete separation of layers. Similarly, Rausell-Colom et al. (1965) suggested that as natural weathering was slow, the replacement of K was not so orderly, and once a particular interlayer region had opened up, continued replacement in that region would be favored over the opening up of the other interlayer region. Thus, the physical action of lichen thalli discussed elsewhere can facilitate and accelerate interlayer K exchange rates. However, according to Gilkes and Suddhiprakarn (1979), packets of a hydrobiotite-like (K-depleted biotite) phase develop within biotite. This process leads to gross exfoliation of mica and the opening of new diffusion avenues. It is reasonable to suspect that the processes discussed above, both the biophysical action of lichens and formation of K-depleted biotite zones, produce more intensive exfoliation.

REFERENCES

AlDahan AA, Morad S. 1986. Chemistry of detrital biotites and their phyllosilicate intergrowths in sandstones. Clays Clay Miner 34:539–548.

Ascaso C. 1985. Structural aspects of lichens invading their substrata: Surface physiology of lichens. Madrid: Universidad Complutense. p 87–113.

Ascaso C, Galvan J, Ortega C. 1976. The pedogenic action of *Parmelia conspersa,* Rhizocarpon geographicum and Umbilicaria postulata. Lichenologist 8:151–171.

Ascaso C, Galvan J. 1976. Studies of the pedogenic action of lichen acids. Pedologia 16:321–331.

Ascaso C, Brown DH, Rapsch S. 1986. The ultrastructure of the phycobiont of dessicated and hydrated lichens. Lichenologist 18:37–46.

Ascaso C, Wierzchos J. 1994. Structural aspects of the lichen-rock interface using back-scattered electron imaging. Botan Acta 107:251–256.

Barshad I, Kishk FM. 1968. Oxidation of ferrous iron in vermiculite and biotite alters fixation and replaceability of potassium. Science 162:1401–1402.

Barth TW. 1948. Oxygen in rocks. A basis for petrographic calculations. J Geol 56:50–61.

Craw D, Coombs DS, Kawachi Y. 1982. Interlayered biotite-kaolin and other altered biotites, and their relevance to the biotite isograd in eastern Otago, New Zealand. Mineral Mag 45:79–85.

Dreher P, Niederbudde AE. 1994. Potassium release from micas and characterization of the alteration products. Clay Miner 29:77–85.

Gilkes RJ. 1973. The alteration products of potassium depleted oxybiotite. Clays Clay Miner 21:303–313.

Gilkes RJ, Young RC, Quirk JP. 1973. Artificial weathering of oxidized biotite—I. Potassium removal by sodium chloride and sodium tetraphenylboron solutions. Soil Sci Soc Am Proc 37:25–28.

Gilkes RJ, Suddhiprakarn A. 1979. Biotite alteration in deeply weathered granite. I and II. Clays Clay Miner 27:349–367.

Goulding KWT. 1983. Thermodynamics and potassium exchange in soils and clay minerals. Adv Agron 36:215–264.

Iskandar IK, Syers JK. 1972. Metal-complex formation by lichen compounds. J Soil Sci 23:255–265.

Jones D, Wilson MJ. 1985. Biomineralization in crustose lichens: Biomineralization in lower plants and animals. Oxford: Clarenton Press. p 91–101.

Joy DC. 1991. An introduction to Monte Carlo simulation. Scanning Microscopy 5:329–337.

Lineares J, Caballero E, Reyes E, Huertas F. 1987. Trace element mobility in bentonite formation: The practical applications of trace elements isotopes to environmental biogeochemistry and mineral resources evaluation. Athena: Theophrastus Publishers. p 233–250.

Morad S. 1990. Mica alteration reactions in Jurassic reservoir sandstones from the Haltenbanken area, Offshore Norway. Clays Clay Miner 38:584–590.

Mortland MM, Lawton K, Uehara G. 1956. Alteration of biotite to vermiculite by plant growth. Soil Sci 82:477–481.

Pozzuoli A, Viela E, Franco E, Ruiz-Amil A, De la Calle C. 1994. Weathering of biotite to vermiculite in quaternary lahars from Monti Ernici, central Italy. Clay Miner 27:175–184.

Rausell-Colom JA, Sweatman TR, Wells CB, Norrish K. 1965. Studies in the artificial weathering of mica: Experimental pedology, Proc. Univ. Nottingham 11th Easter Sch. Agric Sci. p 40–72.

Reichenbach H, Graf von, Rich CI. 1969. Potassium release from muscovite as influenced by particle size. Clays Clay Miner 17:23–29.

Rich CI. 1972. Potassium in soil minerals: Potassium in soil, Proc. 9th. Int. Potash Inst., Landshut, Germany. p 7–24.

Robertson ID, Eggleton RE. 1991. Weathering of granitic muscovite to kaolinite and halloysite and of plagioclase-derived kaolinite to halloysite. Clays Clay Miner 39:113–126.

Ross GJ, Rich CI. 1974. Effect of oxidation and reduction on potassium exchange of biotite. Clays Clay Miner 22:355–360.

Scott AD, Amonette J. 1988. Role of iron in mica weathering: Iron in soils and clay minerals. Dordrecht: D. Reidel. p 537–624.

Stoch L, Sikora W. 1976. Transformations of micas in the process of kaolinization of granites and gneisses. Clays Clay Miner 24:156–162.

Syers J, Iskandar IK. 1973. Pedogenic significance of lichens: The lichen. New York: Academic Press. p 225–248.

Weed SB, Davey CB, Cook MG. 1969. Weathering of mica by fungi. Soil Sci Soc Am Proc 33:702–706.

White SH, Huggett JM, Shaw HF. 1985. Electron-optical studies of phyllosilicate intergrowths in sedimentary and metamorphic rocks. Mineral Mag 49:413–423.

Wierzchos J, Ascaso C. 1994. Application of back-scattered electron imaging to the study of the lichen-rock interface. J Micros 175:54–59.

Wilson MJ. 1995. Interactions between lichens and rocks, a review. Cryptogam Bot 5:299–305.

Wilson MJ, Jones D. 1983. Lichen weathering of minerals and implication for pedogenesis: Residual deposits: surface related weathering processes and materials. Special Publication of the Geological Society, London: Blackwell. p 5–12.